



## NUMERICAL STUDY OF MIXED CONVECTION FLOW IN A LID

Huda A. Al-Mayahi<sup>1</sup>

<sup>1</sup> Department of Mechanical Engineering, College of Engineering, University of Basrah  
Email: [mohammedkader\\_it@yahoo.com](mailto:mohammedkader_it@yahoo.com)

### ABSTRACT

A numerical investigation of steady laminar mixed convection flow of a Copper-water nanofluid in a lid-driven cavity has been executed. In the present study, the left vertical and inclined walls are heated at constant temperature while the right vertical and inclined right walls are maintained at constant cold temperature. The bottom wall is adiabatic and moving with uniform velocity. The study has been carried out for Rayleigh number  $Ra = 10^4 - 10^6$ , Reynolds number  $Re = 20-100$  and solid volume fraction of Cu nanoparticles  $\phi = 0-0.05$ . The effective viscosity and thermal conductivity of the nanofluid have been calculated by Brinkman and Maxwell-Garnett models, respectively. The results indicated that, the Nusselt number increases with increasing  $Ra$ ,  $Re$  and  $\phi$ .

**KEYWORDS:** Mixed convection; Nanofluid; Lid-driven

## 1. INTRODUCTION

Mixed convection has received a noticeable attraction in research due to its wide application in industry likes, solar collectors, storage of grains, disposing of waste materials, etc. The performance of these devices can be improved by using nanofluids rather than regular fluids. A nanofluid is a base liquid with suspended metallic or non-metallic nanoparticles. Because traditional fluids used for heat transfer applications such as water, mineral oils and ethylene glycol have a rather low thermal conductivity, nanofluids with relatively higher thermal conductivities have attracted enormous interest from researchers due to their potential in enhancement of heat transfer with little or no penalty in pressure drop.

[Ali and Eiyad \(2012\)](#) studied laminar mixed convection flow in single and double – lid driven square cavities filled with water –  $\text{Al}_2\text{O}_3$  nanofluid .The left and right walls of the cavity were kept insulated while the bottom and top walls were maintained at constant temperatures with the top surface being the hot wall. It is found that small Richardson number causes reductions in the average Nusselt number. [Abbasian et al. \(2012\)](#) investigated numerically mixed convection laminar flow around an adiabatic body in a lid-driven enclosure filled with nanofluid ( $\text{Al}_2\text{O}_3$ –water)using variable thermal conductivity and viscosity. The vertical enclosure wall is maintained at constant cold temperature while the horizontal bottom wall is kept at constant hot temperature. The top wall of the enclosure is insulated and moving with uniform velocity. The ratio of body length to the enclosure length is kept constant at 1/3. The study has been carried out for  $\text{Ri}$  (0.01-100),  $\text{Gr}$  (104) and  $\text{Pr}$  (0-0.06). The results showed that, the average  $\text{Nu}$  increased by increasing  $\text{Gr}$  and reduction with  $\text{Ri}$ . [Jami et al. \(2013\)](#) studied numerically the mixed convection in lid- driven partially heated cavities. The results show that, for  $\text{Ri}>1$ , the average  $\text{Nu}$  is relatively low while for  $\text{Ri}<1$  the forced convection becomes dominant and the natural convection weak, as a result of which  $\text{Nu}$  is relatively higher. The heat transfer rate increases with increasing the solid volume fraction of the nanoparticles.

[Sivanandam et al. \(2010\)](#) investigated convection flow and heat transfer behavior of nanofluids with different nanoparticles in a square cavity. The hot left wall temperature is varied linearly with height whereas the cold right wall temperature is kept constant. It was found that, the heat transfer rate increases with increasing the volume fraction of the nanofluid for all types of nanoparticles considered. Also, the increment of  $\text{Nu}$  is strongly dependent on the nanoparticles chosen. Samehand [Mansour \(2012\)](#) investigated numerically the mixed convection flows in a square lid-driven cavity partially heated from below using Cu-water, Ag-water,  $\text{Al}_2\text{O}_3$ -water and  $\text{TiO}_2$ - water nanofluid. The results showed that the increasing the  $\text{Gr}$  leads to decreasing both the activity of the fluid motion and the fluid temperature. However, it increases the corresponding  $\text{Nu}$  by adding  $\text{TiO}_2$  nanoparticles to

the base fluid this gives large value of Nu on the contrary, by adding silver (Ag) nanoparticles to the base fluid this gives small values of Nu.

[Aminossadati and Ghasemi \(2009\)](#) studied numerically the natural convection cooling of a heat source embedded on the bottom wall of an enclosure filled with nanofluids. The top and vertical walls of the enclosure are maintained at a relatively low temperature. The results showed that, the increase in Rayleigh numbers strengthens the natural convection flows, which results in a reduction in heat source temperature. [Sheikhzadeh et al. \(2012\)](#) presented the fluid flow and heat transfer in lid-driven enclosures filled with Cu –nanofluid numerically. The moving vertical walls of the enclosure are maintained at constant temperature. The results showed that by increasing the volume fraction of nanoparticles, the variation of average Nu number on the hot wall is linear in two cases.

[Farhad et al. \(2010\)](#) studied numerically laminar mixed convection flows of a cu-water nanofluid in a square lid-driven cavity. The top and bottom walls are insulated while the vertical walls are different constant temperature. It was found that at a fixed Re number the solid concentration affects the flow pattern and thermal behavior particularly for a higher Ra number.

[Eiyad and chamkha \(2010\)](#) studied natural convection heat transfer characteristics in a differentially heated enclosure filled with CuO-EG-Water nanofluids for different variable thermal conductivity and variable viscosity models. The results showed that, the effect of thermal conductivity models was less significant than the viscosity models at high Rayleigh number. [Mostafa and Seyed \(2012\)](#) investigated natural convection fluid flow and heat transfer inside C-shaped enclosures filled with Cu-water nanofluid. The results found that the mean Nusselt number increased with the increase in Rayleigh number and volume fraction of Cu nanoparticles regardless the aspect ratio of the enclosure. It can be concluded from the survey above, that all the studied geometries are rectangular enclosures. Thus, the present study is dedicated to study the mixed convection in such a hooded rectangular enclosure with base is being moving either to right or left direction. This geometry can be considered as a simulation for a modified solar collector.

## 2. THEORETICAL ANALYSIS

A schematic diagram of the considered model is shown in [Fig. 1](#). It is a two – dimensional enclosure of height H and based length L, ( $L=H$ ) filled with Cu-water nanofluid. The insulated lid-driven bottom wall is sliding at a constant speed [ $+u_0$  for case I and with  $-u_0$  for case II]. The left vertical and inclined walls are heated at constant temperature ( $T_h$ ) while the right vertical and inclined walls are kept at constant cold temperature ( $T_c$ ). The Cu-water nanofluid is assumed Newtonian, incompressible, in thermal equilibrium, and the nanoparticles are kept uniform in shape and size. The

thermo-physical properties of the base fluid and the nanoparticles, presented in Table 1, are considered constant with the exception of its density, which varies according to the Boussinesq approximation. The viscosity of the nanofluid is assumed to be a function of volume fractions of nanoparticles by using Brinkman model, Brinkman (1952).

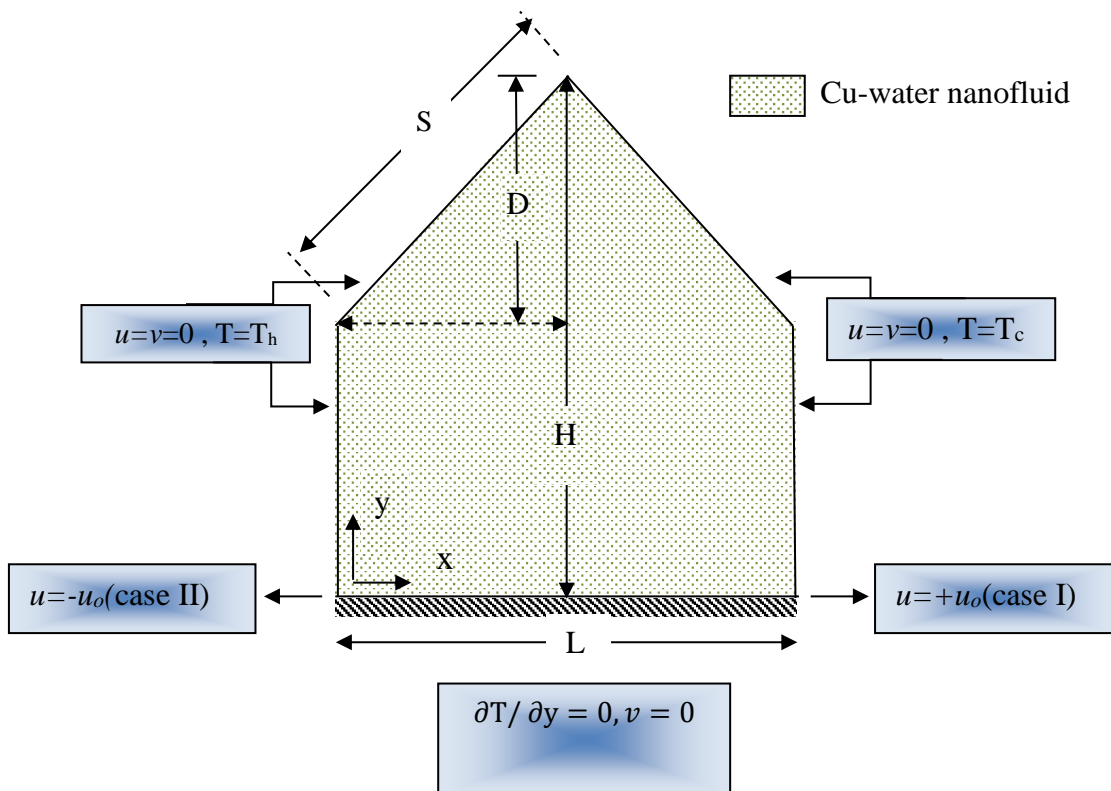


Fig. 1. Schematic diagram of the enclosure.

Table 1. Thermo-physical properties of water and copper Farhad et al., (2010)

Property	Water	Copper
$c_p$	4179	383
$\rho$	997.1	8954
$k$	0.6	400
$\beta$	$2.1 \cdot 10^{-4}$	$1.67 \cdot 10^{-5}$

The governing equations for laminar, steady-state lid driven convection in an enclosure filled with Cu –water nanofluids are given as:

Continuity equation:

$$\frac{\partial u}{\partial x} + \frac{\partial v}{\partial y} = 0 \quad 1$$

Momentum equation in x-direction:

$$u \frac{\partial u}{\partial x} + v \frac{\partial u}{\partial y} = -\frac{1}{\rho_{nf}} \frac{\partial p}{\partial x} + \nu_{nf} \left( \frac{\partial^2 u}{\partial x^2} + \frac{\partial^2 u}{\partial y^2} \right) \quad 2$$

Where:  $\mu_{nf} = \frac{\mu_f}{(1-\phi)^{2.5}}$  and  $\nu_{nf} = \frac{\mu_{nf}}{\rho_{nf}}$

Momentum equation in y-direction:

$$u \frac{\partial v}{\partial x} + v \frac{\partial v}{\partial y} = -\frac{1}{\rho_{nf}} \frac{\partial p}{\partial y} + \nu_{nf} \left( \frac{\partial^2 v}{\partial x^2} + \frac{\partial^2 v}{\partial y^2} \right) + \frac{g}{\rho_{nf}} (T - T_c) [\phi \rho_s \beta_s + (1 - \phi) \rho_f \beta_f] \quad 3$$

Energy equation:

$$u \frac{\partial T}{\partial x} + v \frac{\partial T}{\partial y} = \alpha_{nf} \left( \frac{\partial^2 T}{\partial x^2} + \frac{\partial^2 T}{\partial y^2} \right) \quad 4$$

Where:  $\alpha_{nf} = k_{nf} / (\rho c_p)_{nf}$

The effective density of nanofluid at the reference temperature can be defined as:

$$\rho_{nf} = (1 - \phi) \rho_f + \phi \rho_s \quad 5$$

The heat capacitance of nanofluid can be given as:

$$(\rho C_p)_{nf} = (1 - \phi) (\rho C_p)_f + \phi (\rho C_p)_s \quad 6$$

The effective thermal conductivity of the nanofluid is approximated by the Maxwell – Garnett model [1904]

$$K_{nf} = k_f \left[ \frac{(k_{np} + 2k_f) - 2\phi(k_f - k_{np})}{(k_{np} + 2k_f) + \phi(k_f - k_{np})} \right] \quad 7$$

Equations (1)-(4) can be converted to the dimensionless forms by introducing the following parameters as:

$$X = \frac{x}{H}, Y = \frac{y}{H}, U = \frac{u}{U_0}, V = \frac{v}{U_0}, \theta = \frac{T - T_c}{T_h - T_c}, P = \frac{p}{\rho_{nf} U_0^2} \quad 8$$

Therefore using the above parameters leads to dimensionless form of the governing equations as:

$$\frac{\partial U}{\partial X} + \frac{\partial V}{\partial Y} = 0 \tag{9}$$

$$U \frac{\partial U}{\partial X} + V \frac{\partial U}{\partial Y} = -\frac{\partial P}{\partial X} + \frac{1}{Re} \frac{\rho_f}{\rho_{nf}} \frac{1}{(1-\phi)^{2.5}} \left( \frac{\partial^2 U}{\partial X^2} + \frac{\partial^2 U}{\partial Y^2} \right) \tag{10}$$

$$U \frac{\partial V}{\partial X} + V \frac{\partial V}{\partial Y} = -\frac{\partial P}{\partial Y} + \frac{1}{Re} \frac{\rho_f}{\rho_{nf}} \frac{1}{(1-\phi)^{2.5}} \left( \frac{\partial^2 V}{\partial X^2} + \frac{\partial^2 V}{\partial Y^2} \right) + \frac{Ra}{Re^2 \cdot Pr} \frac{\rho_f}{\rho_{nf}} \left( 1 - \phi + \phi \frac{\rho_s \beta_s}{\rho_f \beta_f} \right) \theta \tag{11}$$

$$U \frac{\partial \theta}{\partial X} + V \frac{\partial \theta}{\partial Y} = \frac{k_{nf}}{k_f} \frac{(\rho C_p)_f}{(\rho C_p)_{nf}} \frac{1}{Re \cdot Pr} \left( \frac{\partial^2 \theta}{\partial X^2} + \frac{\partial^2 \theta}{\partial Y^2} \right) \tag{12}$$

Where:  $Pr = \nu_f/\alpha_f$  ,  $Re = \rho U_o H/\mu$  ,  $Ra = \beta g H^3 \Delta T / (\nu \alpha)$

The boundary conditions are:

$\theta = 1$  ,  $U = V = 0$  for left vertical and inclined walls

$\theta = 0$  ,  $U = V = 0$  for right vertical and inclined walls 13

$\partial \theta / \partial Y = 0$  ,  $V = 0$  ,  $\begin{cases} U = +1 & \text{case I} \\ U = -1 & \text{case II} \end{cases}$  for bottom wall

### 3. NUMERICAL APPROACH

The dimensionless governing equations (9) - (12) with the corresponding boundary conditions given in equation (13) are solved based on the finite element method by using Flex PDE software package. Other useful parameters such as Nusselt number for heated walls can be calculated after solving the governing equations for U, V and  $\theta$ . The local Nusselt numbers for the left vertical and inclined walls are defined as:

$$Nu_l = \frac{K_{nf}}{K_f} \frac{\partial \theta}{\partial X} \Big|_{\text{left vertical wall}} \tag{14}$$

$$Nu_{in} = \frac{K_{nf}}{K_f} \frac{\partial \theta}{\partial n} \Big|_{\text{left inclined wall}} \tag{15}$$

Where n is a normal vector.

The average Nusselt number for each side of the heated walls is determined by integrating the local Nusselt number along the heated walls:

$$Nu_{avl} = \frac{1}{H - D} \int_0^{H-D} Nu_l \cdot dy \tag{16}$$

$$Nu_{avin} = \frac{1}{S} \int_{H-D}^S Nu_{in} \cdot ds \quad 17$$

Where  $s$  is the segment of the inclined wall,  $s = \sqrt{D^2 + (L/2)^2}$

$$L=1, H=1 \text{ and } D=0.5$$

The overall average Nusselt number for the heated walls is be given by:

$$Nu_{avt} = \int_0^{H-D} Nu_l \cdot dy + \int_{H-D}^S Nu_{in} \cdot ds \quad 18$$

#### 4. VALIDATION AND COMPARISON OF THE STUDY

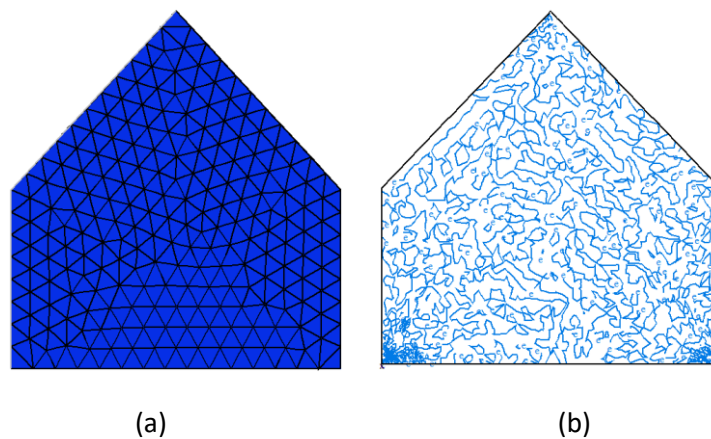
The studied geometry in this paper is an obstructed solar collector cavity; therefore several grid size sensitivity tests together with the continuity equation (  $\frac{\partial U}{\partial X} + \frac{\partial V}{\partial Y} = 0$  ) are achieved. The grid independency test is presented in [Table 2](#). This table shows that the  $Nu_{av}$  becomes stable beyond grid 5. Therefore, the grid 6 (nodes = 3049) is adopted in this paper. The obtained results showed an exactly validation of the velocity distribution for grid size obtained by imposing an accuracy of  $10^{-3}$ . This accuracy is a compromised vale between the result accuracy and the time consumed in each run. The grid domain for  $Ra=104$ ,  $Re=20$  and  $\phi=0$  is shown in [Fig. 2-a](#) and the distribution of  $(\frac{\partial U}{\partial X} + \frac{\partial V}{\partial Y})$  over the domain is presented in [Fig. 2-b](#). [Table .3](#) referred to the comparison of the present values of Nusselt average ( $Nu_{av}$ ) for ( $Ra=104, 105$  and  $106$ ) with the values of reference of [Farhad \(2010\)](#), (third column) and with [De Vahl \(1983\)](#) (fourth column). It is obvious that good agreement is obtained. As a result, the confidence in the present numerical solution is enhanced.

**Table 2. Independency grid test.**

Grid	Nodes	$Nu_{av}$
1	868	5.105
2	1657	5.909
3	2056	6.572
4	2697	7.941
5	2922	8.466
6	3049	8.470

**Table 3. Testing the used code with others.**

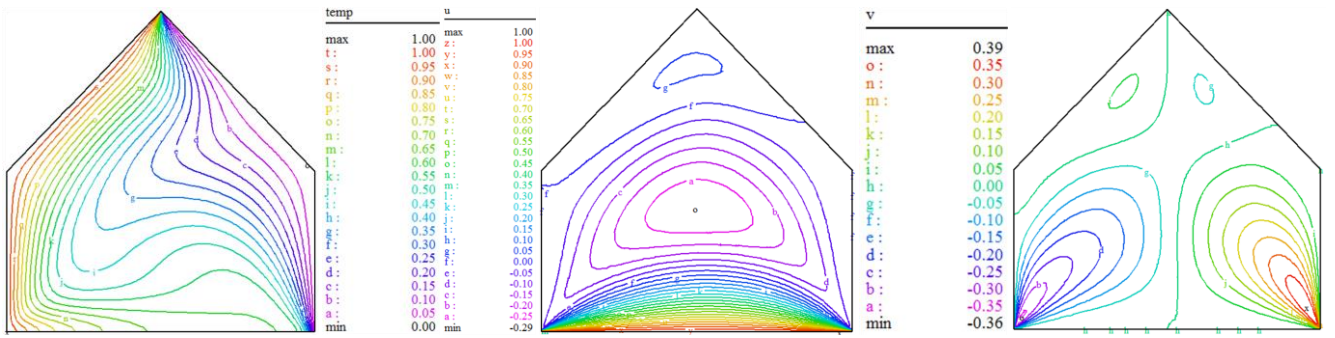
Ra	Nuav				
	Present work	Farhad Talebi et al. [2010]	Error	De Vahl Davis [1983]	Error
104	2.262	2.248	0.006	2.242	0.003
105	4.549	4.503	0.01	4.523	0.006
106	9.183	9.147	0.004	9.035	0.016

**Fig. 2 (a) Grid distribution over the domain (b) validation of continuity equation.**

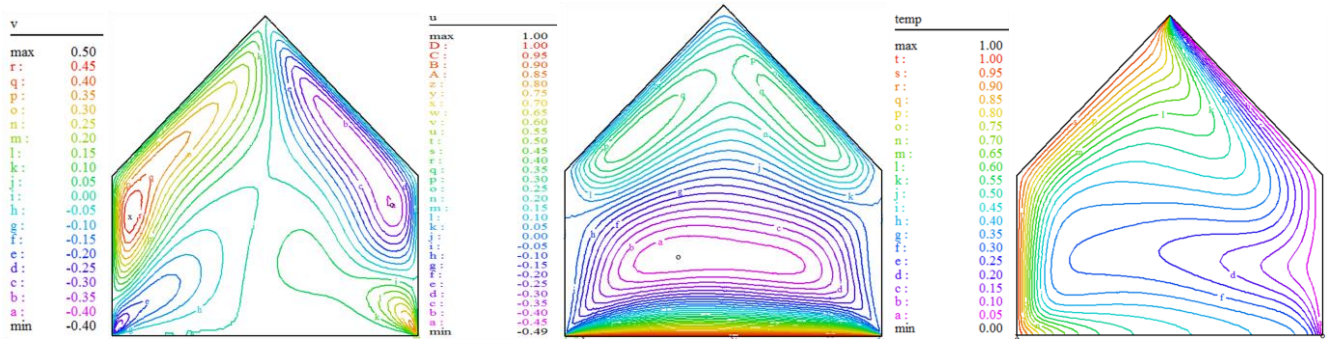
## 5. RESULTS AND DISCUSSIONS

The present study is carried out for copper-water nanofluid flow at Rayleigh number  $Ra=104-106$ , Reynolds number  $Re=1-100$  and solid volume fraction  $\phi=0-0.05$ . The discussion is established on two cases: case I and case II. In case I, the bottom wall is moving to the right while the case II, the bottom wall is moving to the left. Fig. 3 shows isotherms contour (on the left), U-velocity contour (in the middle) and V-velocity contour (on the right) for various Ra numbers,  $Re=20$  and  $\phi=0.05$ . It is noticed that, at lower Ra number the solid concentration has more effect to increase the heat penetration; because the conduction heat transfer effect is overheated with increasing Ra number, so the solid concentration has smaller effect on thermal distribution compared buoyancy effect. When Ra number decreases, the intensity of U –velocity contour increases near the bottom wall due to its moving and buoyancy effect. In addition, V-component increases with increasing Ra number. Fig. 4 indicates the effect of Re number on these contours at  $Ra=104$  and  $\phi=0.05$ , for isotherms as can be seen that when Re number smaller, the effect of lid- driven is insignificant and the intensity of the isotherms are concentrated close to the heated wall.

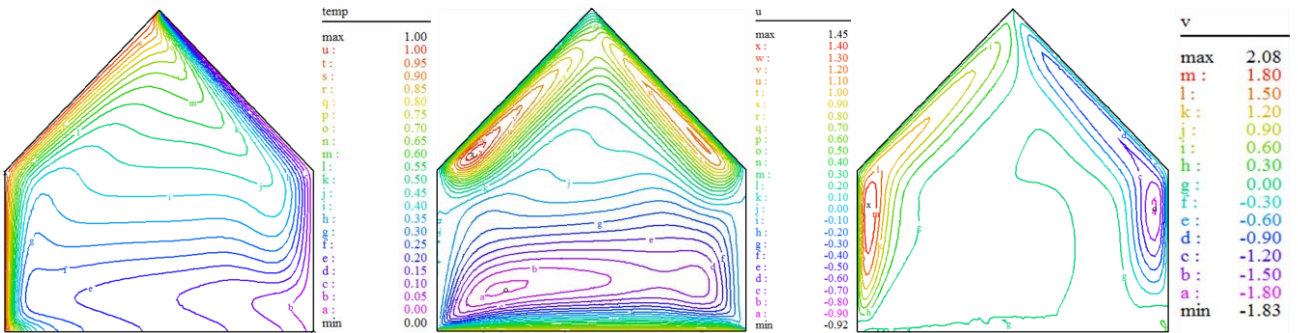




(a) Ra=10<sup>4</sup>

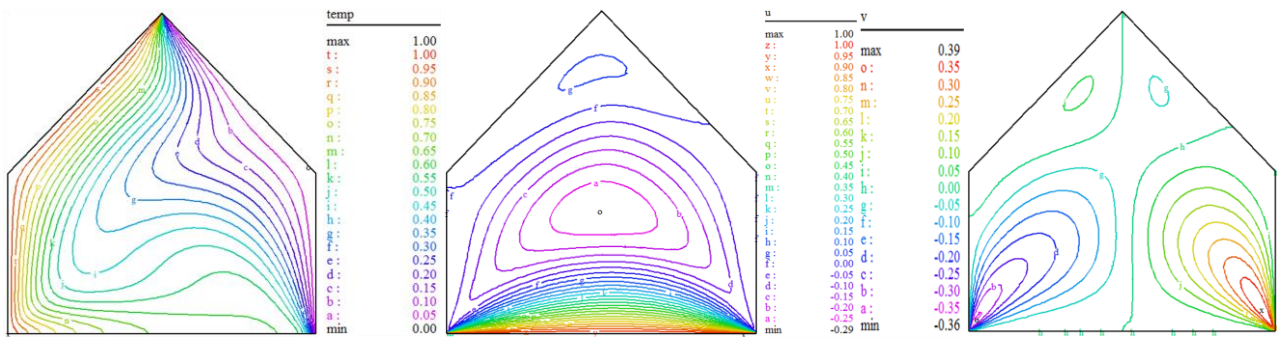


(b) Ra=10<sup>5</sup>

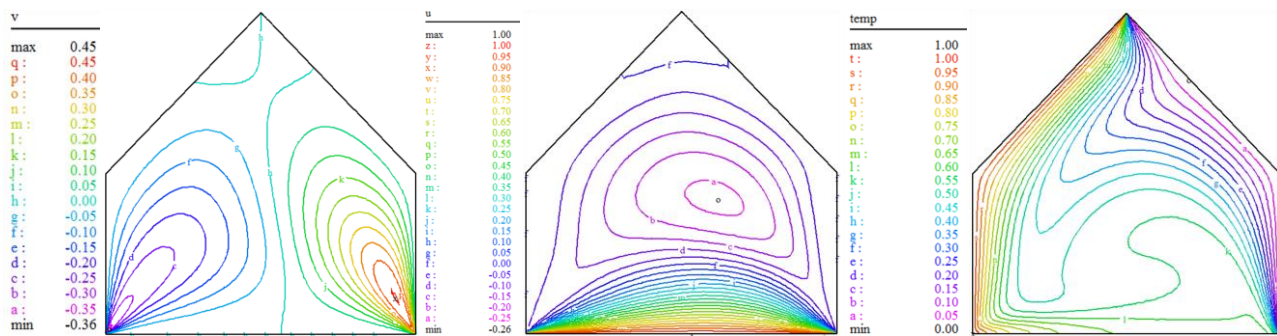


(c) Ra=10<sup>6</sup>

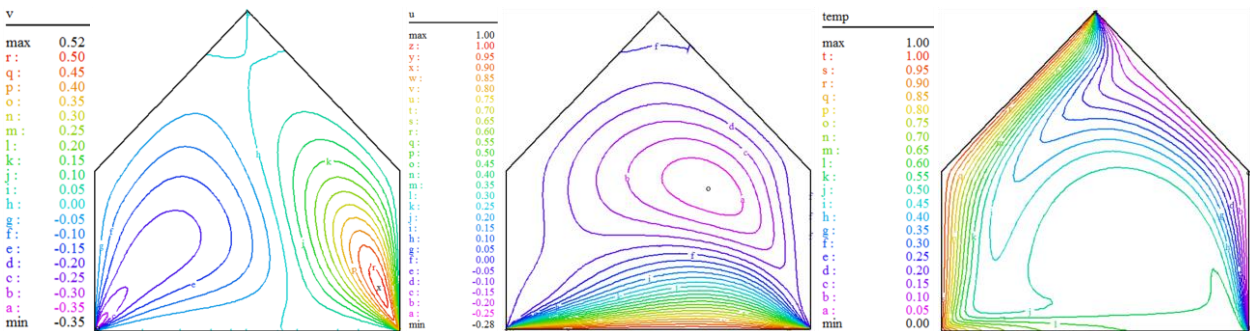
Fig. 3 Isotherms, U-velocity and V-velocity for Re= 20, Ø=0.05 and U=+1 at a) Ra=10<sup>4</sup>, b) Ra=10<sup>5</sup> c) Ra=10<sup>6</sup>.



(a) Re=20



(b) Re=50



(c) Re=100

**Fig. 4 Isotherms, U-velocity and V-velocity for Ra= 104, phi=0.05 and U=+1 at a) Re=20, b) Re=50, c) Re=100.**

However, as Re number increases the effect of lid-driven increases and hence forced convection flow. It is noticed also that with increasing Re, an isothermal zone is localized above the moving bottom wall. At Re=20, the vortex core of U-velocity contour is in the center of the cavity. When Re number increases the vortex core moves to the right side of the cavity due to increasing the forced convection. When Re number increases V-velocity increases as well. Fig. 5 demonstrates the effect of solid volume fraction on this contours at Ra=104 and Re= 20. It is noticed the increase in solid concentration does not have considerable effect on isotherm contour but the intensity of U and V-velocities increases with increasing solid volume fraction due to lid driven flow.

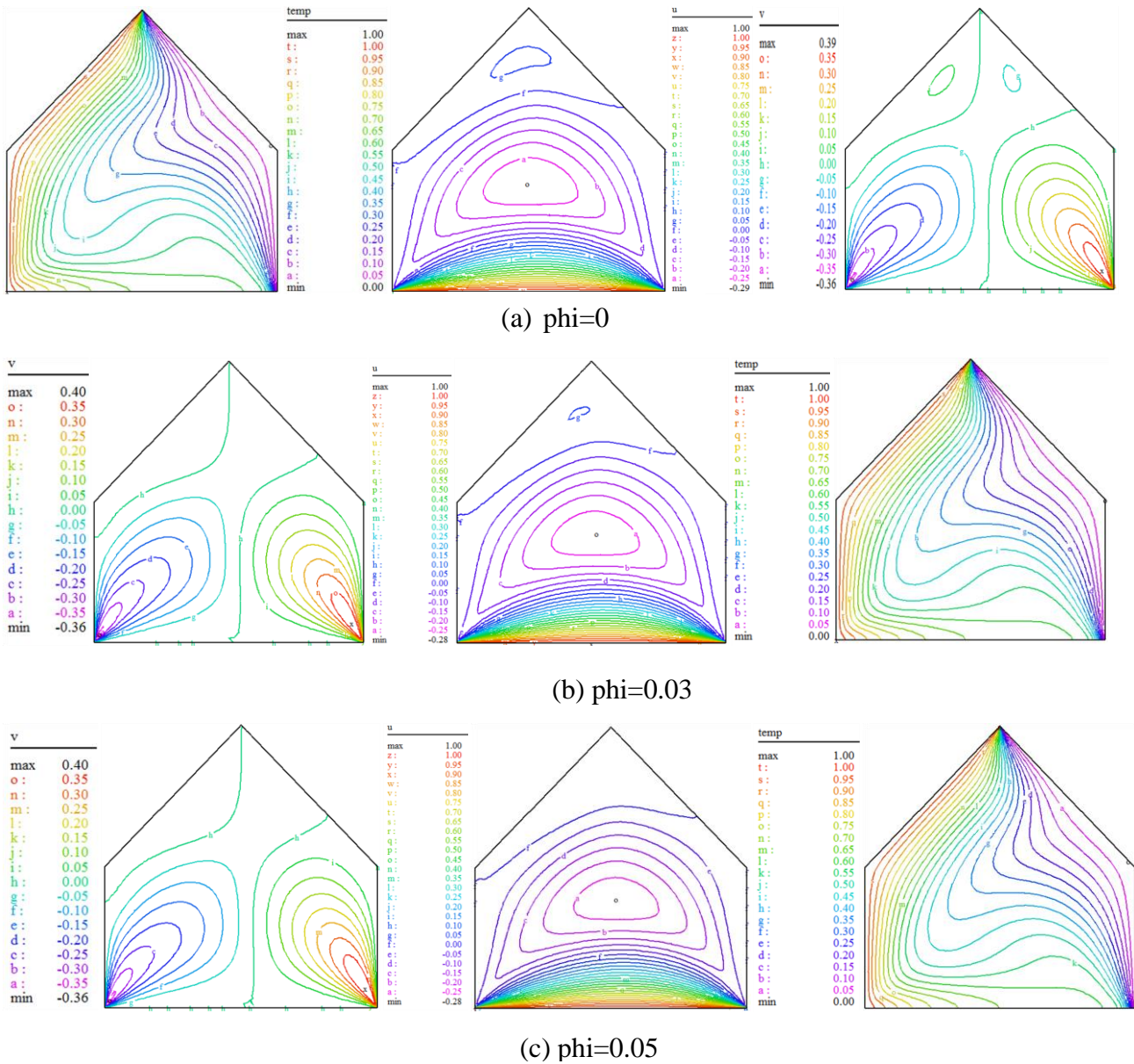
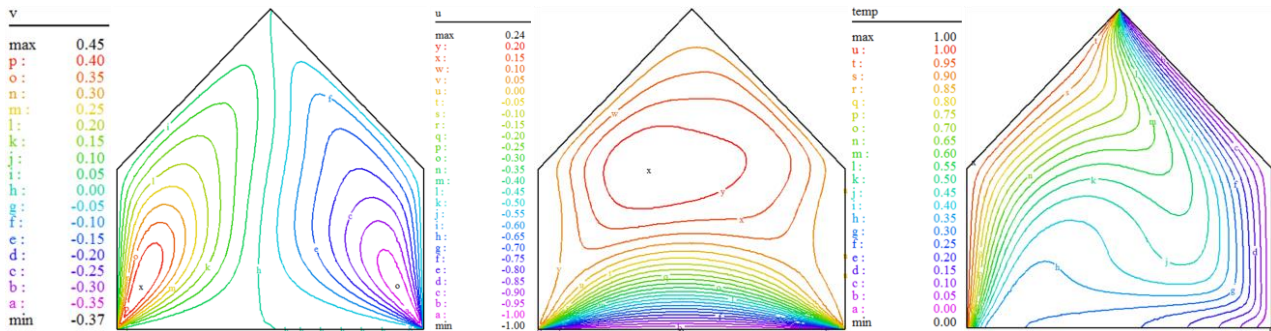


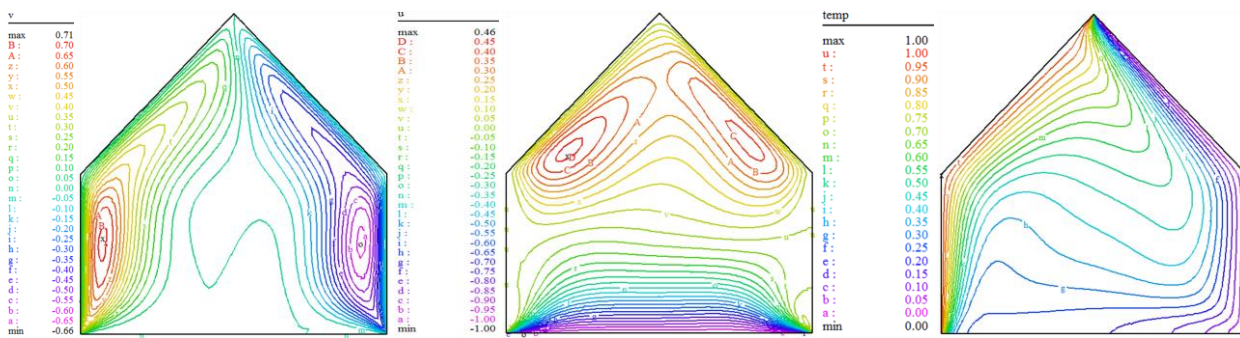
**Fig. 5 Isotherms, U-velocity and V-velocity for  $Ra= 10^4$ ,  $Re=20$  and  $U=+1$  at a)  $\phi= 0$ , b)  $\phi=0.03$ , c)  $\phi=0.05$ .**

Figs. 6 and 7 show for case II, where Fig. 6 demonstrated the effect of variation of  $Ra$  number on the isotherms (left) U-velocity(middle) and V-velocity (right)for  $U=-U$ ,  $Re=20$  and  $\phi=0.05$ . As can be seen for the isotherms, intensity of curves increases near the hot walls with increasing  $Ra$  number. This is an indication of increasing the heat transfer. The isotherms become mostly horizontal with higher  $Ra$ , which means the dominance of natural convection. While at low Rayleigh number ( $Ra = 104$ ), the U-velocity contours show that the nanofluid is mainly subjected to the action of the moving bottom wall, thus, the upper part of the cavity has the same low velocity. When  $Ra$  increases to 105 and further to 106, the effect of natural convection leads to intensified circulation of the nanofluid

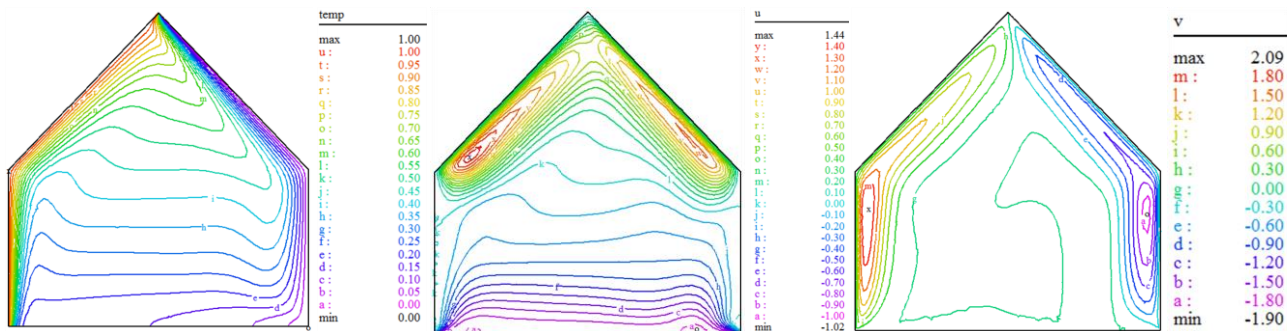
close to the inclined walls. V-component increases with increasing Ra number especially near the hot left sides.



(a)  $Ra=10^4$

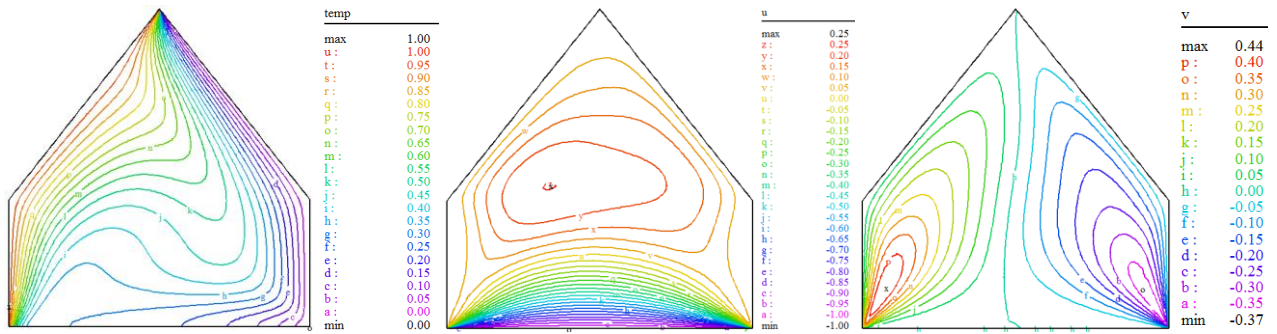


(b)  $Ra=10^5$

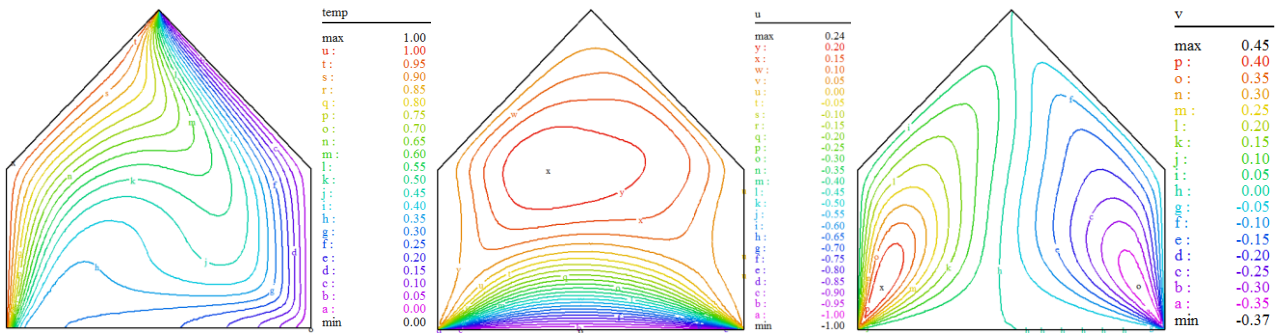


(c)  $Ra=10^6$

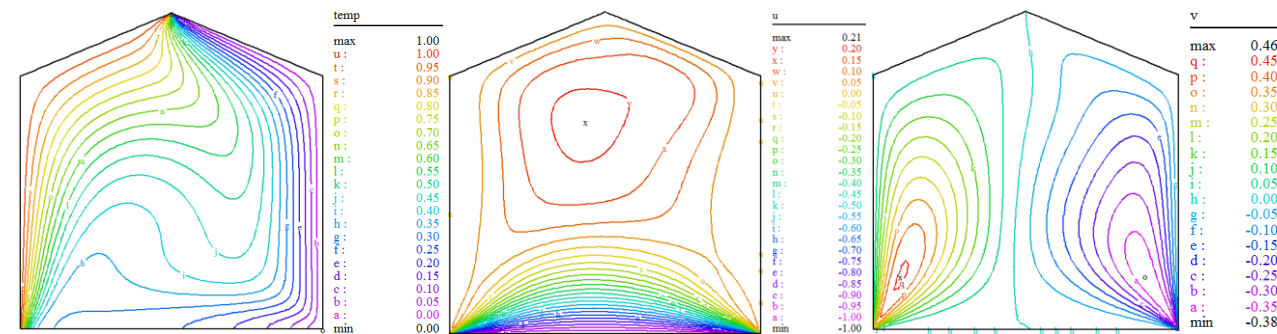
**Fig. 6 Isotherms, U-velocity and V-velocity for  $Re= 20$ ,  $\phi=0.05$  and  $U= -1$  at a)  $Ra=10^4$ , b)  $Ra=10^5$  c)  $Ra=10^6$ .**



(a) D=0.6



(b) D=0.5



(c) D=0.2

**Fig. 7. Isotherms, U-velocity and V-velocity for Ra=10<sup>4</sup>, Re= 20, Ø=0.05 and U= -1 at a) D=0.6, b) D=0.5 c) D=0.**

All these observations are due to the strengthening of the natural convection with increasing Ra. Fig. 7 indicates the effect of the height of the hood of the cavity (D). The isotherms contour do not varied but U-velocity decreased with decreasing value of D while V-velocity increases with decreasing values of D. The attribution of these variations can be referred to the following, when D is decreased, large free path for the vertical component will be available, and therefore, less drag in the vertical path, which leads to enhance the V-component. On the other hand, the behavior of U- component is due to the dominance of V over U components.

Fig. 8 presents that the overall heat transfer ( $Nu_{av}$ ) is an increasing function of  $Ra$ ,  $Re$  and  $\theta$ . Moreover, this figure tell us that when the bottom wall is moving to the left ( $U = -1$ ), the average Nusselt number manifests greater values. This is quite reasonable, because the direction of the lid coincides with the natural movement of nanofluid which is generated from the left walls towards the upper zone of the enclosure, i.e. the aiding mechanism will be obtained  $U = -1$ , and the opposing mechanism is obtained when  $U = +1$ . Fig. 8a-left shows variation of  $Nu_{av}$  on  $Ra$  number for the second case. As a result,  $Nu_{av}$  increases with  $Ra$  number for two cases but the values of  $Nu_{av}$  for cases II larger than case I due to the secondary flow. Fig 8a-right indicates the effect of  $\theta_{av}$  on  $Ra$  for two cases.  $\theta_{av}$  decreases with increasing  $Ra$  number for two cases.

Fig. 8b- left shows the effect of  $Nu_{av}$  on  $Re$  number. As can be seen that  $Nu_{av}$  increases linearly approximately with  $Re$  number for two cases. Fig. 8b-right represents the variation of  $\theta_{av}$  on  $Re$  for two cases. The increase in  $Re$  number leads to decreasing  $\theta_{av}$  for two cases. Fig. 8c-left refers to the effect of  $Nu_{av}$  on  $\theta$ . As can be seen that  $Nu_{av}$  increases  $\theta$  for two cases. Also, that talk for  $\theta_{av}$  at Fig. 8c-right.

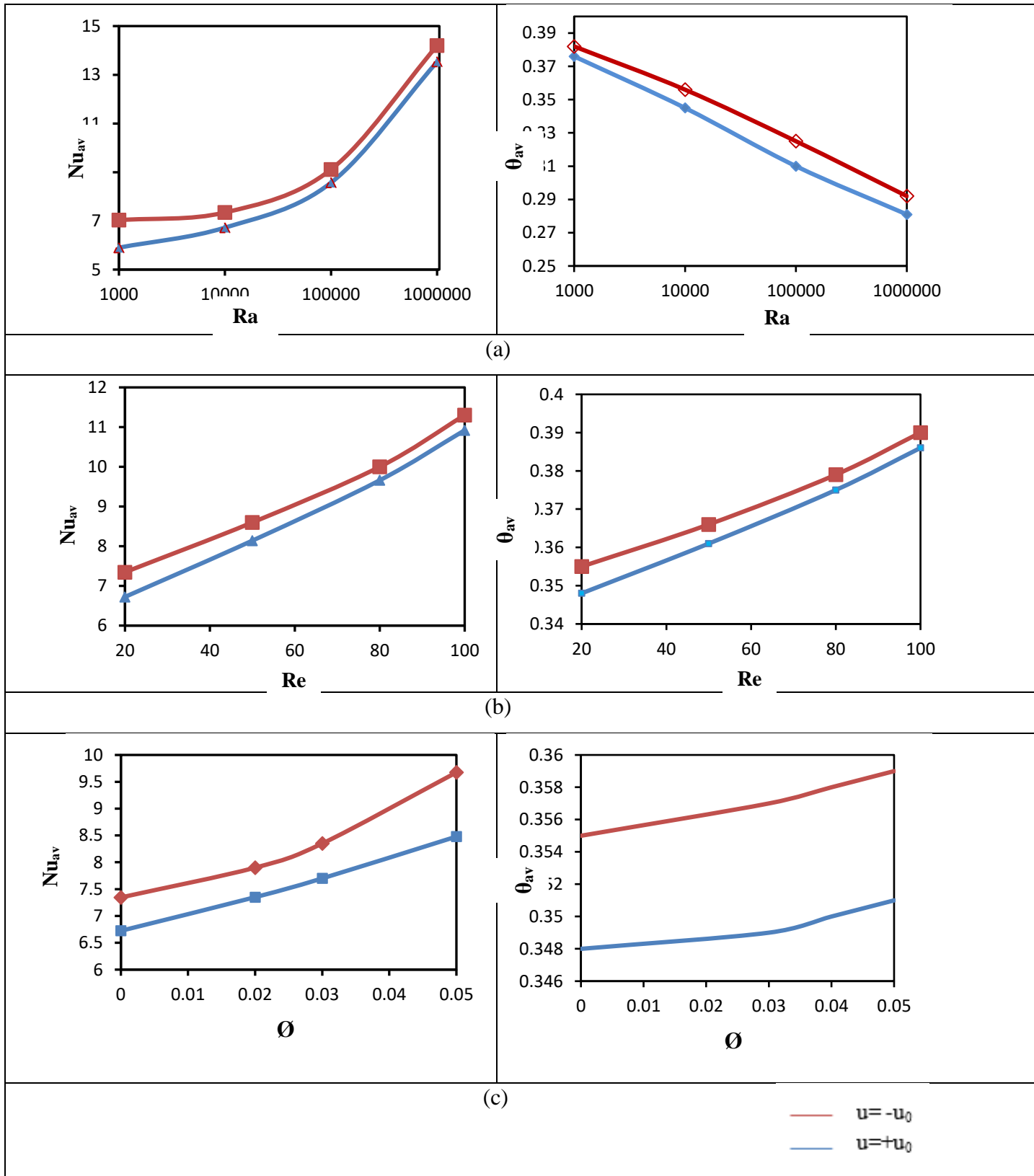


Fig. 8 Variation of Nu<sub>av</sub> and theta<sub>av</sub> with a) Ra , b) Re, c) Phi.

## 6. CONCLUSIONS:

Mixed convection heat transfer of lid driven enclosure filled with Cu-water studied numerically using finite element method implemented in Flex PDE software package. Two cases for lid driven wall [+1 and -1] studied with different ranges of Ra, Re,  $\phi$  and D. The obtained results led us to the following conclusions:

1. Nuav increases with increasing Ra number, Re number and  $\phi$ .
2. Heat transfer inside the enclosure enhanced when the bottom wall is being lid to left, and can be retarded when the bottom wall is being lid to the right ( $U=+1$ ).
3.  $\theta_{av}$  increases with increasing Re number and  $\phi$  for both cases, but decreases with increasing Ra number.

## 7. REFERENCES

Abbasian A.A. , Sheikhzadeh G.A. , Heidary R. , Hajialigol N. & M. Ebrahim Qomi,( 2012) "Numerical study of mixed convection in a lid-driven enclosure with a centered using nanofluid variable properties" . Journal of Nanostructures, JNS 2: pp 51-60.

Ali J. Chamkha &Eiyad Abu-Nada, (2012) "Mixed convection flow in single and double lid-driven square cavities filled with water- Al<sub>2</sub>O<sub>3</sub>nanofluid: Effect of viscosity models". European Journal of Mechanics B/ fluids, 36: pp.82-96.

Aminossadati S.M. and Ghasemi B., (2009) "Natural convection cooling of a localized heat source at the bottom of a nanofluid- filled enclosure". European Journal of Mechanics B/ fluids, 28: PP.630-640.

Brinkman H.C., (1952)" The viscosity of concentrated suspensions and solutions". J. Chem. Phys. 20:pp571-581.

De Vahl Davis G., (1983)" Natural convection of air in a square cavity a benchmark numerical solution ".International Journal of Numerical Methods of Fluids, 3: pp. 249- 264.

Eiyad Abu-Nada and Ali J. Chamkha, (2010)" Effect of nanofluid variable properties on natural convection in enclosures filled with a CuO- EG-Water nanofluid". International Journal of thermal sciences, 49:pp. 2339-2352.



Farhad Talebi, Amir Houshang Mahmoudi and Mina Shahi, (2010) "Numerical study of mixed convection flows in a square lid-driven cavity utilizing nanofluid". *International communications in heat and mass transfer*, 37:pp. 79-90.

Jami Ridha, Brahim Ben-Beya & Taieb Lili, (2013) "Numerical study of mixed convection of nanofluid in lid-driven enclosure partially heated". *International Conference on Control, Engineering & Information Technology (CEIT ' 13)*, Vol.4:pp.223-226.

Maxwell-Garnett, (1904) "Colours in metal glasses and in metallic films". *Philos. Trans. Roy.Soc. A.203*: pp. 385-342.

Mostafa Mahmoodi and Seyed Mohammad Hashemi, (2012)" Numerical study of natural convection of a nanofluid in C-shaped enclosures". *International Journal of thermal sciences*, 55, pp. 76-89.

Sameh E. Ahmed and Mansour M.A., (2012) "Numerical study of mixed convection in partially heated lid- driven cavities filled with nanofluids ". *Int. J. of Appl. Math. and Mech.*, 8(8):pp. 34-54.

Sheikhzadeh G.A., Hajjaligol N., Ebrahim Qomi M. and Fattahi A., (2012)" Laminar mixed convection of Cu-water nanofluid in two-sided lid-driven enclosures". *Journal of Nano structures*: pp. 44-53.

Sivanandam Sivasankarn, Thangaraj Aasaithambi & Subbarayagaunder Rajan, (2010) "Natural convection of nanofluids in a cavity with linearly varying wall temperature". *Maejo Int. J.Sci. Technol.*, 4(03): pp. 468-482.